Metal organic vapor phase epitaxy of InAsP/InP(001) quantum dots for 1.55 μm applications: Growth, structural, and optical properties

A. Michon,[1] R. Hostein,[1] G. Patriarche,[1] N. Gogneau,[1] G. Beaudoin,[1] A. Beveratos,[1] I. Robert-Philip,[1] S. Laurent,[2] S. Sauvage,[2] P. Boucaud,[2] and I. Sagnes[1,a)]
[1]*Laboratoire de Photonique et de Nanostructures, LPN/UPR20—CNRS Route de Nozay, 91460 Marcoussis, France*
[2]*Institut d'Electronique Fondamentale, IEF/UMR8622—CNRS Bâtiment 220, Université Paris Sud, 91405 Orsay, France*

(Received 28 February 2008; accepted 18 June 2008; published online 19 August 2008)

This contribution reports the metal organic vapor phase epitaxy of InAsP/InP(001) quantum dots with a voluntary V-alloying obtained owing to an additional phosphine flux during InAs quantum dot growth. The quantum dots were studied by photoluminescence and transmission electron microscopy. We show that the additional phosphine flux allows to tune quantum dot emission around 1.55 μm while improving their optical properties. The comparison of the optical and structural properties of the InAsP quantum dots allows to deduce their phosphorus composition, ranging from 0% to 30% when the phosphine/arsine flow ratio is varying between 0 and 50. On the basis of the compositions deduced, we discuss on the effects of the phosphine flow and of the alloying on the quantum dot growth, structural, and optical properties. © *2008 American Institute of Physics*. [DOI: 10.1063/1.2968338]

I. INTRODUCTION

Stranski–Krastanow self-assembled III–V quantum dots (QDs) have attracted a lot of attention in the past two decades due to the promising properties of these nanostructures for application on high performance optoelectronic devices. In particular, the maturity of the InAs/GaAs system has led to the fabrication of low threshold and temperature insensitive QD-based lasers emitting at 1.3 μm.[1] Although possible, the extension of their emission wavelength above 1.3 μm remains difficult. The growth of InAs/InP QDs has been developed more recently, motivated by their long emission wavelength that can be tuned to 1.55 μm.[2]

A first difficulty for the growth of InAs/InP QDs is the spontaneous formation of elongated nanostructures (quantum wires or quantum dashes) using molecular beam epitaxy (MBE) on (001)-oriented InP substrates.[3,4] On the contrary, the metal organic vapor phase epitaxy (MOVPE) of InAs on InP spontaneously leads to the formation of QDs.[5–7] As a result, this growth technique appears particularly relevant for QD growth on (001)-oriented InP substrates. A second difficulty in this system is the control of the emission wavelength, since InAs/InP QDs frequently present emission at a greater wavelength than the required 1.55 μm.[8–10] A lot of techniques have been proposed and used to tune their emission toward shorter wavelength. Several studies have shown that the growth of a thin GaAs interlayer under the QDs can lead to a blueshift of the emission.[8] Although this technique has been successfully used to obtain 1.55 μm QD-based lasers,[11] one can think that the GaAs interlayer could damage the efficiency of carrier injection into the QDs. Special capping procedures have also been developed to reduce the emission wavelength. In particular, the double-cap procedure on InAs/InP(113)B QDs grown by MBE allows to tune their emission wavelength to 1.55 μm while reducing the linewidth of their emission down to 50 meV.[2] Such double-capped QDs have allowed to establish the state of the art of QD-based lasers on InP.[12] However, the double-cap procedure on InAs QDs grown on conventional (001)-oriented InP substrates by MOVPE gives rise to important emission linewidth.[13] A similar method, based on the reduction in the cap-layer growth rate,[10,14] also allows to reduce the emission wavelength of InAs/InP(001) QDs, but the emission linewidth remains larger than for double-capped InAs/InP(113)B QDs grown by MBE.

Another way to tune QD emission to shorter wavelength is the intentional alloying of the QD material by incorporating an additional III or V element (III or V alloying). III alloying has been successfully done using $In_{1-x}Ga_xAs$ or $In_{1-x}Al_xAs$ for QD growth on GaAs(001) substrates.[15,16] Maltez *et al.*[17] have also shown the possibility to control emission wavelength using V alloying on $InAs_{1-x}P_x$ QDs grown on GaAs(001) substrates by MOVPE.

Alloying possibilities are reduced for InAs QDs grown on InP substrates due to the small lattice mismatch between QD material and substrate (3.2% instead of 7.2% in the InAs/GaAs system). Actually, Stranski–Krastanow growth mode needs a sufficient lattice mismatch to occur. Theoretical works[18,19] have shown that the critical thickness for Stranski–Krastanow growth transition depends on the lattice mismatch ratio $\Delta a/a$ proportionally to $(\Delta a/a)^{-4}$ or $(\Delta a/a)^{-8}$. Leon *et al.*[15] have experimentally evidenced this increase in the Stranski–Krastanow transition critical thickness when decreasing the lattice mismatch between dot material ($In_{1-x}Al_xAs$) and GaAs substrate. Particularly, for a lattice mismatch smaller than 2.3%, no growth transition is observed. A similar critical lattice mismatch value was also found by Kamath *et al.*[16] for $In_{1-x}Ga_xAs$ QDs grown on

a)Electronic mail: isabelle.sagnes@lpn.cnrs.fr.

GaAs substrates. Enlightened by these results, an ideal InAs*X* alloy for QD emission tuning on InP substrate have to increase its bandgap while maintaining a sufficient lattice mismatch for Stranski–Krastanow transition. Under this point of view, $InAs_{1-x}P_x$ appears as an appellant alloying possibility to control QD emission wavelength. For example, an $InAs_{0.75}P_{0.25}$ alloy would present a bandgap of 620 meV at room temperature (instead of 354 meV for InAs) [20] while keeping enough lattice mismatch (2.4%) for Stranski–Krastanow transition. Another advantage of the phosphorus alloying is that the phosphorus is already present during growth, so the alloying would not strongly modify the growth mechanisms of the QDs. In spite of its potential and of its apparent simplicity, very few works have been done on the growth of InAsP/InP(001) QDs.[6,21] In the only two precedent works, the evidences of phosphorus incorporation into the QDs were given by optical characterizations by means of photoluminescence (PL) using Ge detector with a cutoff around 1.6 μm, so that the PL spectra presented in these studies could be cut by the Ge detector, not giving evidence of phosphorus incorporation into the QDs.

This letter reports the growth by MOVPE of $InAs_{1-x}P_x$/InP(001) QDs with a voluntary V alloying obtained by adding a phosphine flux during InAs QD growth. This additional phosphine flux allows to tune QD emission wavelength to 1.55 μm while improving their optical properties. The optical study by PL and the structural characterizations by transmission electron microscopy (TEM) allow to deduce the compositions of the QDs in part III, and in part IV, to discuss on the effects of the phosphine flux and of the alloying on the QD growth, structural, and optical properties.

II. EXPERIMENTS

The samples were grown in a vertical-reactor low-pressure MOVPE system using hydrogen as carrier gas and standard precursors [arsine (AsH_3), phosphine (PH_3), and trimethylindium (TMI)]. The reference sample (sample A1) was grown using the following growth sequence. First, a 250 nm thick InP buffer layer was grown at 650 °C on an InP(001) substrate. Then, the growth temperature was ramped down to 510 °C for the QD growth. The QDs were formed by a 18 s InAs deposition under an arsine flow rate of 10 SCCM (SCCM denotes cubic centimeter per minute at STP) and an hydrogen-diluted TMI (hereafter called TMI) flux of 50 SCCM. This TMI flux leads to an InAs growth rate of 0.4 ML/s, and then to a nominal thickness of InAs deposition of 7.2 ML (1 ML$\approx$0.3 nm). Without growth interruption, the QDs were covered by a 60 nm thick InP cap layer grown under a phosphine flux of 300 SCCM and a TMI flux of 50 SCCM (growth rate of 0.2 ML/s).

Samples B1–F1 were grown with identical conditions than for sample A1, except that a phosphine flux was added during the InAs deposition while keeping constant the arsine flux at 10 SCCM. The phosphine flux was adjusted to correspond to PH_3/AsH_3 ratios of 5, 20, 30, 40, and 50 for samples B1, C1, D1, E1, and F1, respectively. We have also grown two samples with a reduced cap-layer growth rate. Samples A2 and D2 are similar to samples A1–D1, respectively, except that the QDs were embedded with a cap-layer growth rate of 0.05 ML/s (instead of 0.2 ML/s for the other samples). The growth conditions are summarized in Table I.

TABLE I. PH_3/AsH_3 ratios and cap-layer growth rates of the studied samples.

Sample	PH_3/AsH_3 ratio	Cap-layer growth rate (ML/s)
A1	0	0.2
B1	5	0.2
C1	20	0.2
D1	30	0.2
E1	40	0.2
F1	50	0.2
A2	0	0.05
D2	30	0.05

The room temperature PL spectra were obtained using a Fourier transform infrared spectrometer with a cooled MCT detector (cutoff around 10 μm), while the optical excitation was provided by the 514 nm line of an Ar laser. The low temperature (77 K) PL spectra were obtained using a grating monochromator with a cooled Ge detector (cutoff around 1.6 μm), while the optical excitation was provided by the 532 nm line of a doubled Nd:yttrium aluminum garnet laser. The TEM views were obtained on a Philips CM20 working with an acceleration voltage of 200 kV. The samples were mechanically and chemically thinned down to 200 nm before observations. The thinning was completed with ionic thinning for cross-section observations.

III. OPTICAL AND STRUCTURAL CHARACTERIZATIONS: DETERMINATION OF THE QDS COMPOSITIONS

Normalized room temperature PL spectra of samples A1–F1 are presented in Fig. 1(a). The emission of sample A1 (grown without phosphine flux during QD growth) is centered around 660 meV. When adding an increasing additional phosphine flux during QD growth, the emission is shifted toward high energy and reaches 910 meV for a PH_3/AsH_3 ratio of 50 (the fine structure of the emission from sample F1 will be discussed later). By varying the PH_3/AsH_3 ratio during QD growth, the emission can be tuned around 1.55 μm (800 meV). The linewidth (measured at half maximum) and the integrated intensity corresponding to the spectra presented in Fig. 1(a) are plotted as a function of the PH_3/AsH_3 ratio in Fig. 1(b). When increasing the PH_3/AsH_3 ratio, the integrated intensity increases, reaches a maximum, and decreases, while the linewidth follows an opposite behavior. Sample D1, obtained with a PH_3/AsH_3 ratio of 30, presents an intense emission peaked at 780 meV (1.59 μm) with a reduced linewidth of 80 meV (160 nm). A first result of this study is that an additional phosphine flux during InAs QD growth allows to tune QD emission to the technologically important wavelength of 1.55 μm while improving their optical properties for applications.

The strong blueshift of the emission observed when adding a phosphine flux during QD growth can be due to an increase in the bandgap of the material forming the QDs due

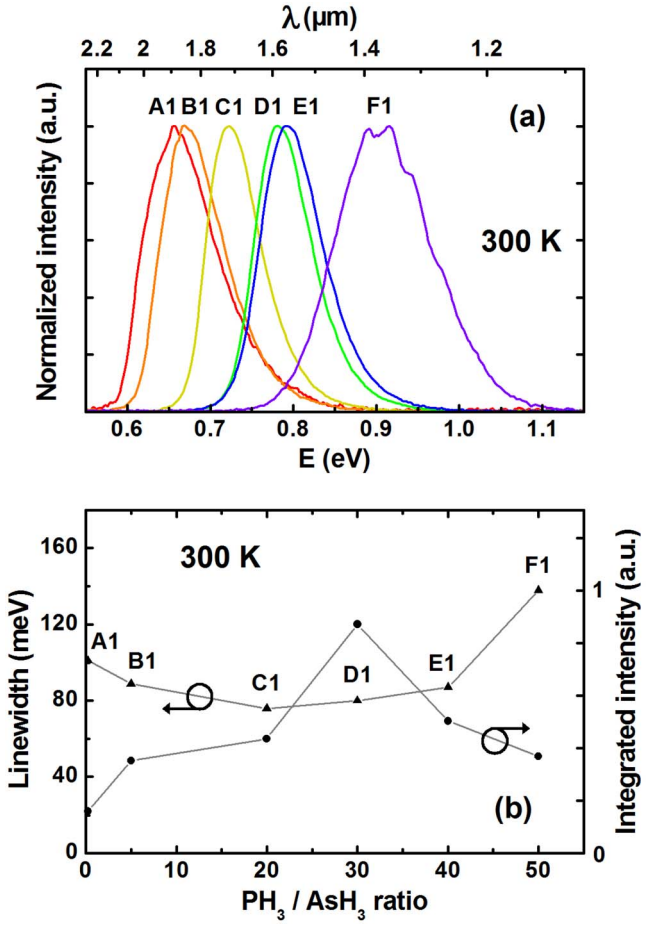

FIG. 1. (Color online) (a) Normalized room temperature PL spectra of samples A1–F1 and (b) corresponding linewidth (▲) and integrated intensity (●) as a function of the PH_3/AsH_3 ratio. Samples A1–F1 were obtained with PH_3/AsH_3 ratio ranging from 0 to 50 during QD growth.

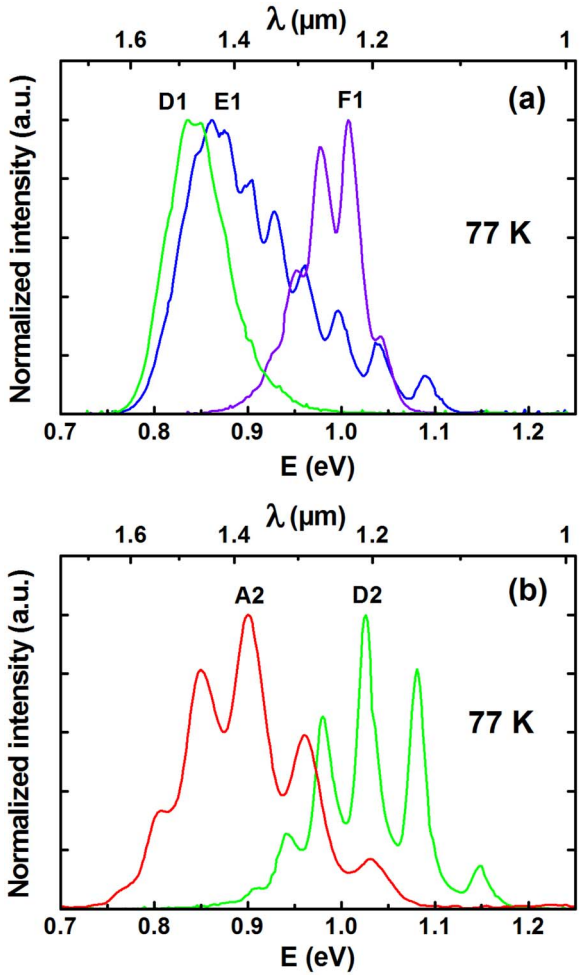

FIG. 2. (Color online) (a) Normalized low-temperature (77 K) PL spectra of samples D1–F1 and (b) of samples A2 and D2. Samples A2 and D2 are similar to samples A1 and D1, respectively, except that the QDs were capped with a lower cap-layer growth rate (0.05 ML/s instead of 0.2 ML/s).

to phosphorus incorporation into the QDs. Nevertheless, the behavior shown in Fig. 1 is not sufficient to prove it. The additional phosphine flux could have some other important effects affecting the sizes and shapes of the QDs, in addition, or not to a bandgap increase. Even in the case where there is no phosphorus incorporation into the QDs, the increase in the phosphine flux can, for example, modify the diffusivity of the adatoms[22,23] (kinetics effects) or the surface energy[7] (thermodynamics effects). A phosphorus incorporation will also modify surface and elastic energies. The modification of the elastic energies, due to the reduction in the lattice mismatch, could increase the critical thickness and decrease the QD density.[18,19] In this case, the reduction in the QD density would be correlated with an increase in the QD sizes, and finally to a decrease in their emission energies, contrary to what is hunted. Elsewhere, the irregular variation of the optical properties (Fig. 1) seems to indicate that many effects occur when the phosphine flow is varying. In the following, we present further optical and structural characterizations to discuss on the effects of the phosphine flux on the QD growth and on their properties.

The room temperature PL spectrum of sample F1 [Fig. 1(a)] presents a peak structure due to the emission of QD families with height varying by monolayer steps. Such peak structure has already been observed and described in several studies of InAs/InP(001) quantum wires or quantum dashes grown by MBE (Refs. 3 and 24) and InAs/InP(001) QDs grown by chemical beam epitaxy[14] or MOVPE.[13,25,26] In particular, Refs. 25 and 26 give clear demonstrations on the basis of the comparison of the luminescence and of the structural properties studied either by TEM (Ref. 25) or by scanning transmission microscopy.[26] The peak structure observed on room temperature PL spectrum of sample F1 appears more precisely at low temperature [Fig. 2(a)] due to the reduction in the thermal spreading of the emission from a single QD family. The emission from QD families with height varying by monolayer step is characteristic of QDs presenting low aspect ratios and flat interfaces. In the case of InAs(P)/InP(001) QDs, the monolayer stepping is mainly due to the desorption of integer monolayers on the top of the QDs during cap-layer growth[27] that gives very flat and well defined top interfaces.[26] The bottom interface is also flat but less well defined, as commonly observed for standard bidimensional growth. It is well known that the emission energy of low aspect ratio QDs can be approximated by the emission energy of a quantum well with the same thickness and composition than that of the QDs.[13,25] We can compare the calculated emission energies from $InAs_{1-x}P_x/InP$ quantum

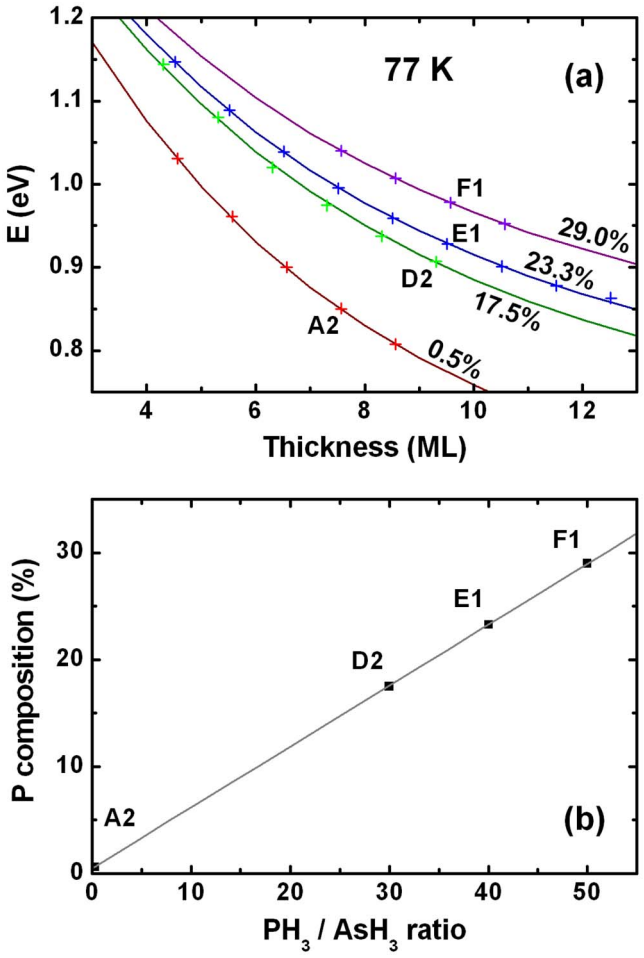

FIG. 3. (Color online) (a) Comparison of the emission energy of the QD families (cross marks) observed on the low temperature PL spectra of samples A2, D2, E1, and F1 (see Fig. 2) to the theoretical emission energy of $InAs_{1-x}P_x/InP$ quantum wells (continuous lines) as a function of the thickness. The compositions of the quantum wells have been adjusted to deduce the composition of the QDs. (b) Composition of the QDs deduced from Fig. 3(a) as a function of the PH_3/AsH_3 ratio during QD growth.

wells to the emissions from different QD families with thickness varying by monolayer step, as expressed by $h=h_0+i\times a$, with h_0 an height offset, i an integer, and a the thickness of 1 ML. We have plotted in Fig. 3(a) the calculated emission energy of an $InAs_{1-x}P_x/InP$ quantum well (eight band **k.p** calculus taking into account strain effects[28]) with a phosphorus composition of $x=29.0\%$. We have also plotted, as cross marks, the emission energies from the four different peaks which were resolved on the low temperature PL spectrum of sample F1 [Fig. 2(a)]. There is a unique set of quantum well composition x and QD height offset h_0 which allows to match the emission energies. In this case, the heights are supposed varying between 7.6 and 10.6 ML. The use of noninteger QD heights is justified by the presence of a gradual interface under the QDs. This simple method evidences the phosphorus incorporation into the QDs and gives moreover an estimation of their composition.

Figure 2(a) also presents the low temperature PL spectra of samples D1 and E1. The well defined fine structure of the spectrum from sample E1 also allows to deduce the composition of the QDs of this sample in the same way presented above for sample F1. We obtain a phosphorus composition of $x=23.3\%$ [emission energy versus thickness are plotted on Fig. 3(a)]. The low temperature PL spectrum of sample D1 presents only two peaks. We did not observe peak structure for samples A1–C1 principally due to the narrowing of the QD family emission energy spacing toward shorter energies. To deduce the composition of the QDs in the same way that presented above, we need to observe a peak structure due to the emission of QD families. We have studied the low temperature PL of samples A2 and D2 [plotted in Fig. 2(b)], similar to samples A1 and D1, except that the QDs of these samples were capped using a smaller cap-layer growth rate. It has led to a decrease in the QD heights, so that their emissions are shifted toward higher energies.[10,27] The broadening of the QD family emission energy spacing toward high energies allows to distinguish the different QD families. It is now possible to estimate the compositions of the QDs of samples A2 and D2 in the same way than presented above. It gives phosphorus compositions $x=0.5\%$ and $x=17.5\%$ for samples A2 and D2, grown under PH_3/AsH_3 ratios of 0 and 30. The emission energies of the QD families and of the quantum wells are plotted on Fig. 3(a). As will be verified in the following, the reduction in the cap-layer growth rate does not modify the composition of the dots, especially for the low growth temperature used for QDs and cap-layer growth, so that the composition of the QDs into A1 and D1 would be identical than those into A2 and D2, respectively.

We have plotted the phosphorus composition of the QDs deduced above as a function of the PH_3/AsH_3 ratio in Fig. 3(b). As can be seen, the phosphorus composition is proportional to the PH_3/AsH_3 ratio during QD growth. The excellent alignment of the experimental points corroborates the reproducibility and the reliability of our method. However, we have to remind that this method is based on the comparison of the emission energy of the QD families with the calculated emission energies of quantum wells assuming abrupt interfaces. The effects of the smooth lower interfaces or of the lateral confinement in the QDs could create gradual deviations of the emission energy between QD families and quantum wells, so that the error on the phosphorus composition could be greater than expected from the good match between experimental and theoretical plots on Fig. 3(a).

The increase in the PH_3/AsH_3 ratio leads to a greater phosphorus incorporation. We have to notice that significant phosphorus incorporation requires high PH_3 flux: a PH_3/AsH_3 ratio of 50 gives a phosphorus incorporation of 29% (sample F1). This is due to the poor cracking efficiency of the phosphine compared to that of the arsine at the low growth temperature used.[23] We also notice that the higher phosphorus incorporation ($x=29\%$) obtained for sample F1 corresponds to a lattice mismatch between QD material and substrate of 2.3%. This lattice mismatch is near the lower limit of lattice mismatch allowing Stranski–Krastanow transition in Refs. 15 and 16. Finally, the phosphorus incorporation evidenced here leads to an increase in the bandgap of the material forming the QDs. Thus, it is at least partly responsible for the increase in the emission energy observed above. In the following, we will study the structural properties of

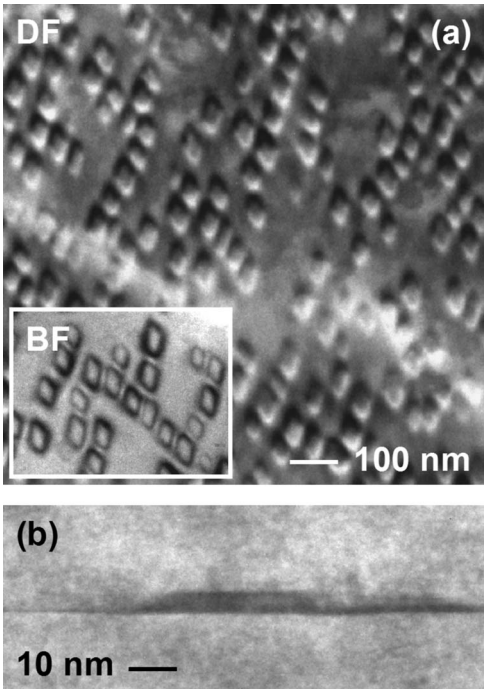

FIG. 4. Typical TEM micrographs of the reference sample A1. (a) Plane view in 220 DF condition. (inset) BF condition. (b) 002 DF condition TEM cross section.

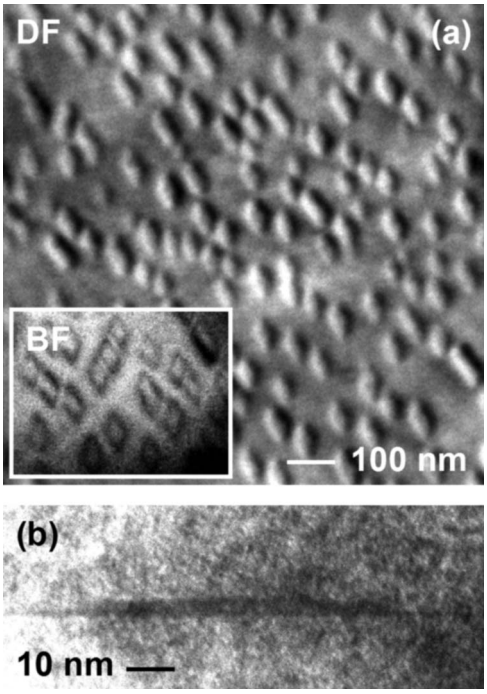

FIG. 5. Typical TEM micrographs of sample D1, grown with a PH_3/AsH_3 ratio of 30 during QD growth. (a) plane view in 220 DF condition. (Inset) BF condition. (b) 002 DF condition TEM cross section.

the InAsP/InP(001) QDs in order to discuss on the other effects of the phosphine flow on the QD growth and properties.

We have studied using TEM the reference sample A1 (no phosphine flow during QD growth) and sample D1, containing QDs emitting around 1.55 μm (PH_3/AsH_3 ratio of 30 during QD growth). TEM plane views were obtained using 220 dark field (DF) and bright field (BF) under 001 zone axis imaging conditions, and cross-section micrographs were obtained using 002 DF imaging condition (we conventionally consider the growth direction as a [001] crystallographic direction). Figures 4(a) and 5(a) present 220 DF TEM plane views from samples A1 and D1. BF TEM plane views are presented in the insets. Figures 4(b) and 5(b) present cross-section TEM micrographs of two typical QDs of samples A1 and D1. Table II summarizes the measured structural properties. The main difference between the two samples is that sample A1 contains a low density of plastically relaxed QDs (slightly less than 1×10^8 cm^{-2}, not shown here), while sample D1 is defect-free. We also observe an increase in the wetting-layer thickness, from 0.8 nm for sample A1 to 1.5 nm for sample D1 (experimental uncertainty about 0.3 nm). Otherwise, the two samples contain QDs with similar morphological properties, although their emissions are clearly different. First of all, the two samples contain about the same QD densities within the estimated errors: 1.47×10^{10} cm^{-2} for sample A1 and 1.44×10^{10} cm^{-2} for sample D1 (error of $\pm0.05\times10^{10}$ cm^{-2}). The QDs of the two samples present a parallelogram shape with sides along the $[1\bar{3}0]$ and $[3\bar{1}0]$ crystallographic directions, as already observed for InAs/InP(001) QDs grown using MOVPE.[29,30] We have measured the lateral sizes perpendicularly to the $[1\bar{3}0]$ and $[3\bar{1}0]$ QD edges on BF TEM views, as described in Ref. 30. The average lateral sizes are $W_{min}=30.6$ nm and $W_{max}=36.7$ nm for sample A1 and $W_{min}=33.5$ nm and $W_{max}=42.3$ nm for sample D1 (about 40 QDs measured on each sample; experimental uncertainty on the average lateral sizes about 0.5 nm). Finally, we have measured the heights of the QDs on cross-section views (about 15 QDs measured on each samples). The mean QD heights (including wetting-layer thickness) are about the same, 3.9 nm for sample A1 and 3.8 nm for sample D1 (uncertainty on the average heights about 0.3 nm), while the height dispersions slightly decrease, from 0.70 nm for sample A1 to 0.55 nm for sample D1.

TABLE II. Structural properties of the QDs from sample A1 and sample D1 (TEM measurements). Uncertainties are indicated after the symbol "±."

Sample	PH_3/AsH_3 ratio	QD density	Average QD widths		Average QD height (nm)	QD height dispersion (nm)	Wetting layer thickness (nm)
			W_{min} (nm)	W_{max} (nm)			
A1	0	$(1.47\pm0.05)\times10^{10}/cm^2$	(30.6 ± 0.5)	(36.7 ± 0.5)	(3.9 ± 0.3)	0.7	(0.8 ± 0.3)
D1	30	$(1.44\pm0.05)\times10^{10}/cm^2$	(33.5 ± 0.5)	(42.3 ± 0.5)	(3.8 ± 0.3)	0.55	(1.5 ± 0.3)

These structural characterizations are coherent with the phosphorus incorporation into the QDs evidenced before. First, we observe that while the two samples contain QDs with similar shape and sizes, only sample A1 contains plastically relaxed QDs. This indicates that the material forming the QDs of sample D1 is less stressed than the material forming the QDs of sample A1. An increasing phosphorus incorporation will reduce the lattice mismatch between QD material and substrate and then reduce the strain from sample A1 to sample D1. The increase in the wetting-layer thickness from sample A1 to sample D1 is also coherent with the expected increase in the critical thickness for Stranski–Krastanow growth transition when decreasing the lattice mismatch between QD material and substrate.[18,19] The comparison of the optical and structural properties of samples A1 and D1 also evidences the phosphorus incorporation. Actually, the blueshift of the emission when increasing the PH_3/AsH_3 ratio can only be explained by a phosphorus incorporation into the QDs of sample D1, since samples A1 and D1 present very similar morphological properties, and more particularly, about the same average heights. Furthermore, we can estimate the composition of the alloy forming the QDs by comparing the emission energies observed on PL spectra and the mean QD heights deduced from cross-section TEM views. The QDs of the two samples present low aspect ratios of about 0.12. The low aspect ratios allow to calculate the emission energy of the QDs using a quantum well model. We have calculated the emission energies of quantum wells with different compositions, and thicknesses equals to the mean QD heights of samples A1 and D1. The calculated emission energies using compositions of the well of $x=2.5\%$ for sample A1 and $x=17.9\%$ for sample D1 produce a good match with the energies of the peaks observed on room temperature PL spectra (656 and 781 meV for samples A1 and D1, respectively). These compositions match the compositions deduced from the study of the low temperature PL spectra of samples A2 and D2 ($x=0.5\%$ and $x=17.5\%$, respectively). The small phosphorus incorporation into the QDs of samples A1 and A2 is due to the presence of residual phosphine during QD growth. Finally, the good match between the compositions deduced in two different ways validates the adequacy of these methods to deduce the composition of the dots. This also indicates that the cap-layer growth does not significantly affect the compositions of the QDs, as expected for the low growth temperature used for QD growth.

IV. DISCUSSION ON THE EFFECTS OF PHOSPHINE FLOW ON QDS GROWTH, STRUCTURAL, AND OPTICAL PROPERTIES

We have evidenced phosphorus incorporation into the InAs QDs when adding a phosphine flux and deduced their composition by two different ways. This allows to discuss on the effects of the phosphine flow and of the alloying on the QD growth, structural, and optical properties.

Under III element-limited growth conditions, the growth rate is proportional to the III element flow rate.[23] The QDs in samples A1–F1 were obtained using a TMI flux of 50 SCCM. In our growth conditions, this TMI flow rate added to an arsine flow leads to an InAs growth rate of 0.40 ML/s. The same TMI flow rate added to a phosphine flow leads to an InP growth rate of 0.20 ML/s. This difference between InAs and InP growth rates under III element-limited growth conditions can be due to the complex interactions between precursors at different steps of their pyrolysis, as frequently observed in MOVPE. Under phosphine and arsine flow, we expect that the $InAs_{1-x}P_x$ growth rate *GR* is proportional to the As and P compositions of the alloy grown,

$$GR_{InAs_{1-x}P_x} = (1-x)\cdot GR_{InAs} + x\cdot GR_{InP}.$$

This gives for sample D1 ($x=17.5\%$) an InAsP growth rate of about 0.36 ML/s. Consequently, the QDs of sample D1 were grown with a nominal thickness of 6.5 ML, slightly less than for sample A1 (7.2 ML). Elsewhere, we observe on the cross-section TEM views that the wetting-layer thickness increases from 0.8 nm (2.7 ML) for sample A1 to 1.5 nm (5.0 ML) for sample D1. Consequently, the additional phosphine flux leads to a decrease in the amount of material for QD formation, on one hand due to the decrease in the InAsP growth rate (decrease of about 0.7 ML), and on the other hand due to the increase in the wetting-layer thickness (increase of about 2.3 ML). This decrease in the amount of material for QD formation (from 4.5 ML for sample A1 to 1.5 ML for sample D1) could result in a decrease in the QD density.[9,31,32] Moreover, some theoretical and experimental works have shown that the decrease in the lattice mismatch between QD material and substrate leads to a decrease in the QD density.[18,19] Contrary to what is expected from these results, the density is quite unchanged from sample A1 to sample D1, although their compositions correspond to lattice mismatch decreasing from 3.2% to 2.7%. Kinetic effects, such as a reduction in the diffusivity of the adatoms due to the occupation of surface sites by V elements,[22] could explain the absence of density decrease from sample A1 to sample D1.

The precise shape of the QDs after their formation remains difficult to know, especially for InAs(P)/InP QDs grown by MOVPE. On one hand, the shape and the heights of the QDs can be strongly changed during temperature decay (for uncapped samples[25]) or during overgrowth (for capped samples[10,33]). On the other hand, the lack of *in situ* growth monitoring in MOVPE impedes to check such evolutions. Despite of these difficulties, we can discuss on the shape of InAs(P)/InP QDs on the basis of the structural characterizations presented above. We have evidenced that the nominal thickness of InAsP contributing to the formation of the QDs decreases from 4.5 to 1.5 ML from sample A1 to sample D1, while the QD density remains quite unchanged. It indicates that the volume of InAs(P) for the formation of each QD is decreased from sample A1 to sample D1. We have also observed a slight increase in the lateral sizes of the QDs from sample A1 to sample D1 (of about 13%). Only a decrease in the QD heights (before cap-layer growth) from sample A1 to sample D1 can be coherent with the expected decrease in the volume of the QDs. The reduction in the QD heights, and consequently of their aspect ratios, could be due to the apparition of shallow facets on the top of the QDs. High aspect ratios for QDs generally allow to have an im-

portant lateral strain relaxation, on the cost of the formation of steep facets. It is not surprising that the reduction in the lattice mismatch between QD material and substrate—and consequently of the strain in the QDs—promotes the reduction in the QD aspect ratios, possibly by the formation of shallower facets on the top of the QDs.

We notice that while the qualitative material balance indicates that the QD heights before cap-layer growth decrease from sample A1 to sample D1, cross-section TEM observations of the capped samples have shown about the same QD heights. Once again, we have to remind that the cap-layer growth strongly affects the QD morphology in the InAs(P)/InP system, and that the capped QDs studied here have undergone a strong decrease in their heights during overgrowth. A smaller desorption of the top of the InAsP QDs during overgrowth compared to that for "pure" InAs QDs could explain the lack of QD height variations from sample A1 to sample D1, contrary to what was expected from the material balance.

We have observed a small reduction in the linewidth of the emission from sample A1 to sample D1 [Figs. 1(a) and 1(b)]. This is coherent with the slight decrease in the height dispersions from sample A1 to sample D1 evidenced by the TEM study. The reduction in the height dispersion could be partly due to the reduction in the aspect ratio of the QDs, especially in the case of the apparition of shallow facets on the top of the QDs when the lattice mismatch is decreased. However, we observe an increase in the linewidth of the emission on the PL spectra from sample D1 to sample F1. In particular, we can count on the low temperature PL spectra the number of QD families, the heights of which are varying by monolayer steps. We count about 2, 8, and 5 QD families on samples D1, E1, and F1, respectively. We believe that both the QD heights and the height dispersions before cap-layer growth are monotonically decreasing with the PH_3/AsH_3 ratio increase, and that the increase in the height dispersions observed on the capped samples D1–F1 [Figs. 1(a) and 1(b)] is due to cap-layer growth effects occurring on smaller QDs. Such complex cap-layer effects (observed, for example, on the PL spectra of samples D1 and D2, containing identical QDs embedded with different cap-layer growth rates) are beyond the scope of this study and will be discussed elsewhere.[10] In summary, we suggest that both heights and height dispersions of the QDs are decreased when increasing phosphorus incorporation. The reduction in the height dispersion is preserved by the cap-layer growth for the thickest QDs (samples A1–D1), but cap-layer growth effects are occurring on thinnest QDs (samples D1–F1), leading to an increase in their height dispersions.

We can finally discuss on the evolution of the integrated intensity of the QD emission when their energy is changed due to the phosphorus incorporation. Figure 1(b) presents the integrated intensity of the room temperature PL spectra as a function of the PH_3/AsH_3 ratio using a low excitation intensity of about 50 W/cm^2, an excitation intensity for which we do not observe a saturation of the emission. We observe an increase in the intensity from sample A1 to sample D1 and a decrease from sample D1 to sample F1. Since structural characterizations have shown that the density is almost unchanged from sample A1 to sample D1, we think that the efficiency of the emission is increased from sample A1 to sample D1. The decrease in the intensity from sample D1 to sample F1 could be due to the increase in thermally activated escape of the holes from QD states toward wetting-layer states or due to a decrease in the QD density. Further optical characterizations are in progress and will be presented elsewhere.

V. CONCLUSION

We have grown InAsP/InP(001) QDs with a voluntary phosphorus incorporation using MOVPE. The structural and optical properties of the InAsP/InP(001) QDs have been studied using PL and TEM characterizations. We first show that PH_3/AsH_3 ratio between 0 and 50 during QD growth allows to grow QDs with phosphorus composition between 0% and 30%. We have discussed on the various effects occurring due to the phosphine flux and to the phosphorus incorporation into the QDs. The interpretation of the observations involves kinetic effects due to the additional phosphine flow, energetic effects due to the reduction in the lattice mismatch between QD material and substrate, and capping-layer growth effects. The phosphorus incorporation allows to tune QD emission to shorter wavelength while decreasing the linewidth and increasing the intensity of the emission. In particular, a PH_3/AsH_3 ratio of 30 allows to obtain a high density (about 1.5×10^{10} cm^{-2}) of InAsP QDs (phosphorus composition about 18%) presenting an intense emission around 800 meV (1.55 μm) with a reduced linewidth of 80 meV.

AKNOWLEDGMENTS

This work was supported by the SANDIE EC Network of Excellence, by SESAME Project No. 1377, by the Région Ile de France, and by the Conseil Général de l'Essonne.

[1] T. J. Badcock, R. J. Royce, D. J. Mowbray, M. S. Skolnick, H. Y. Liu, M. Hopkinson, K. M. Groom, and Q. Jiang, Appl. Phys. Lett. **90**, 111102 (2007).
[2] C. Paranthoen, N. Bertru, O. Dehaese, A. Le Corre, S. Loualiche, B. Lambert, and G. Patriarche, Appl. Phys. Lett. **78**, 1751 (2001).
[3] J. Brault, M. Gendry, G. Grenet, G. Hollinger, Y. Desières, and T. Benyattou, Appl. Phys. Lett. **73**, 2932 (1998).
[4] J. M. García, L. González, M. U. González, J. P. Silveira, Y. González, and F. Briones, J. Cryst. Growth **227–228**, 975 (2001).
[5] H. Marchand, P. Desjardins, S. Guillon, J.-E. Paultre, Z. Bougrioua, R. Y.-F. Yip, and R. A. Masut, Appl. Phys. Lett. **71**, 527 (1997).
[6] N. Carlsson, T. Junno, L. Montelius, M.-E. Pistol, L. Samuelson, and W. Seifert, J. Cryst. Growth **191**, 347 (1998).
[7] G. Saint-Girons, A. Michon, I. Sagnes, G. Beaudoin, and G. Patriarche, Phys. Rev. B **74**, 245305 (2006).
[8] S. Anantathanasarn, R. Nötzel, P. J. van Veldhoven, T. J. Eijkemans, and J. H. Wolter, J. Appl. Phys. **98**, 013503 (2005).
[9] T. Okawa, Y. Yamauchi, J. Yamamoto, J. Yoshida, and K. Shimomura, J. Cryst. Growth **298**, 562 (2007).
[10] A. Michon, G. Patriarche, G. Beaudoin, G. Saint-Girons, N. Gogneau, S. Laurent, S. Sauvage, P. Boucaud, and I. Sagnes (unpublished).
[11] S. Anantathanasarn, R. Nötzel, P. J. van Veldhoven, F. W. M. van Otten, Y. Barbarin, G. Servanton, T. de Vries, E. Smalbrugge, E. J. Geluk, T. J. Eijkemans, E. A. J. M. Bente, Y. S. Oei, M. K. Smit, and J. H. Wolter, Appl. Phys. Lett. **89**, 073115 (2006).
[12] E. Homeyer, R. Piron, F. Grillot, O. Dehaese, K. Tavernier, E. Macé, J. Even, A. Le Corre, and S. Loualiche, Jpn. J. Appl. Phys., Part 1 **46**, 6903 (2007).

[13]Y. Sakuma, M. Takeguchi, K. Takemoto, S. Hirose, T. Usuki, and N. Yokoyama, J. Vac. Sci. Technol. B **23**, 1741 (2005).
[14]P. J. Poole, R. L. Williams, J. Lefebvre, and S. Moisa, J. Cryst. Growth **257**, 89 (2003).
[15]R. Leon, S. Fafard, D. Leonard, J. L. Merz, and P. M. Petroff, Appl. Phys. Lett. **67**, 521 (1995).
[16]K. Kamath, P. Bhattacharya, and J. Phillips, J. Cryst. Growth **175–176**, 720 (1997).
[17]R. L. Maltez, E. Ribeiro, W. Carvalho, Jr., D. Urgate, and G. Medeiros-Ribeiro, J. Appl. Phys. **94**, 3051 (2003).
[18]C. W. Snyder, J. F. Mansfield, and B. G. Orr, Phys. Rev. B **46**, 9551 (1992).
[19]B. J. Spencer, P. W. Worhees, and S. H. Davis, J. Appl. Phys. **73**, 4955 (1993).
[20]I. Vurgaftman, J. R. Meyer, and L. R. Ram-Moham, J. Appl. Phys. **89**, 5815 (2001).
[21]F. E. Faradjev, Mater. Sci. Eng., B **94**, 243 (2002); **95**, 279 (2002).
[22]K. Yamaguchi, K. Yujobo, and T. Kaizu, Jpn. J. Appl. Phys., Part 2 **39**, L1245 (2000).
[23]G. B. Stringfellow, *Organometalic Vapor-Phase Epitaxy: Theory and Practice* (Academic, San Diego, 1989).
[24]B. Alén, J. Martínez-Pastor, A. García-Cristobal, L. González, and J. M. García, Appl. Phys. Lett. **78**, 4025 (2001).
[25]A. Michon, I. Sagnes, G. Patriarche, G. Beaudoin, M. N. Mérat-Combes, and G. Saint-Girons, J. Appl. Phys. **100**, 033508 (2006).
[26]Y. Akanuma, Y. Yamakawa, Y. Sakuma, T. Usuki, and A. Nakamura, Appl. Phys. Lett. **90**, 093112 (2007).
[27]A. Michon, Ph.D. thesis, Université Paris 6, 2007.
[28]J-M. Gérard, Ph.D. thesis, Université Paris 6, 1990.
[29]H. Hwang, S. Yoon, H. Kwon, E. Yoon, H.-S. Kim, J. Y. Lee, and B. Cho, Appl. Phys. Lett. **85**, 6383 (2004).
[30]A. Michon, I. Sagnes, G. Patriarche, G. Beaudoin, M.-N. Mérat-Combes, and G. Saint-Girons, Phys. Rev. B **73**, 165321 (2006).
[31]K. Kawaguchi, M. Ekawa, A. Kuramata, T. Akiyama, H. Ebe, M. Sugawara, and Y. Arakawa, Appl. Phys. Lett. **85**, 4331 (2004).
[32]B. Bansal, M. R. Gokhale, A. Bhattacharya, and B. M. Arora, J. Appl. Phys. **101**, 094303 (2007).
[33]A. Michon, G. Patriarche, G. Beaudouin, G. Saint-Girons, N. Gogneau, and I. Sagnes, Appl. Phys. Lett. **91**, 102107 (2007).